WAVEGUIDE INVARIANT FOCUSING FOR BROADBAND ADAPTIVE BEAMFORMING IN A SHALLOW WATER CHANNEL

Hailiang Tao and Jeffrey L. Krolik

Department of Electrical and Computer Engineering
Duke University, Durham, NC, 27708
Email: {ht10, jk}@ee.duke.edu

ABSTRACT

Focusing methods are effective broadband techniques that can reduce the observation time required for adaptive beamforming. However, often focusing methods designed for planewave signals do not prevent broadband covariance matrix rank inflation for shallow-water multipath wavefronts. The waveguide invariant is a robust channel parameter that describes the dispersive characteristics of an oceanic waveguide. Using the relationship between the waveguide invariant and horizontal wavenumber differences, this paper introduces a new broadband waveguide invariant focusing (WIF) method that can mitigate rank inflation for multipath signals. The new WIF method involves summing narrowband snapshots from array apertures which are judiciously shifted as a function of frequency. The shifted apertures may be obtained naturally as a result of towed horizontal array motion or via sub-aperture processing of a fixed long array. Simulation results for WIF against end-fire interference in a shallow-water waveguide are given to illustrate the performance improvement against conventional approaches.

***Index Terms*—** Array signal processing, Sonar signal processing, Direction of arrival estimation

1. INTRODUCTION

Broadband beamforming and spatial spectral estimation are important steps in passive source detection and localization. Processing broadband signals by combining a series narrowband adaptive beamformer outputs is straightforward but requires long observation times to estimate adaptive weights of each frequency. The focusing approach [1, 2] was introduced to combine data snapshot outer products ”coherently” across the frequency band. By preprocessing the sensor outputs, focusing techniques try to transform the signature of broadband targets from multiple-rank models into ”coherent” rank-one models. This reduction of dimensionality shortens minimum observation time and lowers the threshold signal-to-noise ratio (SNR). Earlier work concerns focusing broadband planewaves. For example, the Coherent Signal-Subspace (CSS) method [1] aligns the signal subspace of each narrowband covariance matrices with that of a reference frequency. This method requires a preliminary estimate of target directions. The STeered Covariance Matrix (STCM) method [2] achieves focusing by inserting delays on snapshots corresponding to each steering direction, avoiding the need to make an initial estimation. In shallow water acoustic waveguides, coherent multipath results in non-plane-wavefronts which do not remain rank one using conventional focusing methods. The resulting rank inflation using larger bandwidths thus challenge the direct extension of planewave focusing techniques on ocean acoustic propagation models.

The waveguide invariant β is a channel parameter describing the dispersive characteristics of a stratified oceanic waveguide. It governs a simple relationship between frequency and range in the spectrogram intensity surface. [3] Some authors have used this relationship to enhance broadband processing via operations on spectrogram intensity surface. [4, 5] Though simple to apply, processing intensity surface typically requires a high SNR.

In this paper, we use the waveguide invariant to achieve focusing for broadband multipath signals. Instead of treating the spectrogram intensity surface, we deal with the set of the narrowband complex data snapshots. We exploit the relationship between waveguide invariant and the frequency dependence of horizontal wavenumber differences. The resulting method, waveguide invariant focusing (WIF), achieves broadband focusing in the same sense as previous focusing techniques do in planewave case, i.e., rank inflation is avoided.

2. WAVEGUIDE INVARIANT FOCUSING FOR ENDFIRE INTERFERENCE SUPPRESSION

Consider the problem of suppressing a loud endfire interference at known range in the context of broadband horizontal array beamforming. Although WIF could be applied to any broadband multipath interfering signal with known range and bearing, near endfire interference, due to bearing spreading across multiple beams, is hard to suppress. As shown in Fig.

Supported by the ONR Code 321US 6.1 sonar signal processing program.

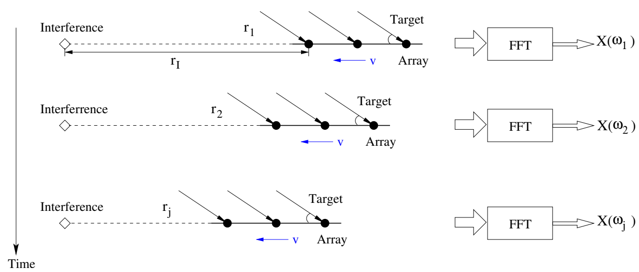

Fig. 1. Broadband beamforming with a close endfire interference

1, assume the towed horizontal linear array is moving along its axis direction. In this scenario, the received signal is a superposition of the broadband multipath interfering signal and the remote target signal, as well as additive white noise. A snapshot at frequency ω_j can be expressed as:

$$\mathbf{x}(\omega_j) = \mathbf{x}_I(\omega_j) + \mathbf{x}_T(\omega_j) + \mathbf{n}_j \tag{1}$$

where $\mathbf{x}_I(\omega_j)$ is the multipath interference. The target $\mathbf{x}_T(\omega_j) = s_T(\omega_j)\hat{\mathbf{v}}$ is a known wavefront multiplied with a complex Gaussian random variable. The noise vector $\mathbf{n}_j$ is spatially white and uncorrelated across frequencies. The interference, target and noise are mutually uncorrelated.

The interfering wavefront $\mathbf{x}_I(\omega_j)$ can be expressed by the normal mode expression:

$$\begin{aligned}\mathbf{x}_I(\omega_j) &= s_I(\omega_j)\sum_m A_m(z_I, z_r)\exp\left(-jk_m(\omega_j)\mathbf{r}_j\right) \\ &= s_I(\omega_j)\exp\left(-jk_1(\omega_j)\mathbf{r}_j\right)\odot \\ &\quad \sum_m A_m(z_I, z_r)\exp\left(-j(k_m - k_1)\mathbf{r}_j\right)\end{aligned} \tag{2}$$

where $s_I(\omega_j)$ is the interference amplitude at frequency ω_j, $A_m(z_I, z_r)$ is mode eigenfunction evaluated at interference depth z_I and receiver depth z_r. k_m is horizontal wavenumber. $\odot$ is the element-by-element Hadamard product. $\mathbf{r}_j$ is the range vector whose elements represent the horizontal distance from the interference to each hydrophone sensor. As will be used below, the subscript j is included to indicate that this distance vector may be frequency-dependent. Let

$$\mathbf{r}_j = r_j^0 + \Delta\mathbf{d} \tag{3}$$

where r_j^0 is the horizontal distance from the interference to the reference sensor. $\Delta\mathbf{d}$ is the array element spacing vector along array axis measuring from the reference sensor.

Grachev [6] found that the waveguide invariant parameter β describe the frequency dependence of horizontal wavenumber differences:

$$\Delta k_{mn} = \zeta_{mn}\omega^{-1/\beta} \tag{4}$$

in which ζ_{mn} is a constant related to mode numbers. (4) suggests that the horizontal wavenumber difference depends on frequency only through β for any combination of mode numbers. The quantity β is found to be approximately constant or invariant for a group of closely spaced modes with respect to frequency and mode wavenumber differences. [3]

Applying (3) and (4) to (2) gives,

$$\begin{aligned}\mathbf{x}_I(\omega_j) &= s_I(\omega_j)\exp\left(-jk_1(\omega_j)(r_j^0 + \Delta\mathbf{d})\right) \\ &\quad \odot\sum_m A_m\exp\left(-j\zeta_{m1}\omega_j^{-1/\beta}\mathbf{r}_j\right) \\ &= \tilde{s}_I(\omega_j)\exp\left(-jk_1(\omega_j)\Delta\mathbf{d}\right)\odot\mathbf{b}_j\end{aligned} \tag{5}$$

where

$$\mathbf{b}_j = \sum_m A_m\exp\left(-j\zeta_{m1}\omega_j^{-1/\beta}\mathbf{r}_j\right) \tag{6}$$

is the interference direction vector demodulated at wavenumber k_1.

In order to focus $\mathbf{b}_j$ across frequencies, we conduct spatial resampling to align all $\mathbf{b}_j$ into a common subspace. We can pick up any reference frequency within the band, but suppose we want to align all $\mathbf{b}_j$ to $\mathbf{b}_1$, the one corresponding to the lowest frequency ω_1. This means adapting $\mathbf{r}_j$ according to frequency ω_j to satisfy:

$$\omega_j^{-1/\beta}\mathbf{r}_j = \omega_1^{-1/\beta}\mathbf{r}_1.$$

Let $\mathbf{r}_1 = r_I + \Delta\mathbf{d}$, where r_I is the interference horizontal distance. Define $\left(\frac{\omega_j}{\omega_1}\right)^{1/\beta} = \eta_j$, we have:

$$\mathbf{r}_j = r_I + (\eta_j - 1)r_I + \eta_j\Delta\mathbf{d} \tag{7}$$

By satisfying (7), $\mathbf{b}_j = \mathbf{b}_1 = \mathbf{b}$, then we can rewrite the interference signal $\mathbf{x}_I(\omega_j)$ as:

$$\mathbf{x}_I(\omega_j) = \tilde{s}_I(\omega_j)\exp\left(-jk_1(\omega_j)\Delta\mathbf{d}\right)\odot\mathbf{b} \tag{8}$$

Next, assume we have knowledge of the first wavenumber k_1 at each frequency, we can perform the usual presteering to eliminate its frequency dependence:

$$\hat{\mathbf{x}}_I(\omega_j) = \exp\left(jk_1(\omega_j)\Delta\mathbf{d}\right)\odot\mathbf{x}_I(\omega_j) = \tilde{s}(\omega_j)\mathbf{b} \tag{9}$$

Thus, after spatial resampling and presteering, the direction vector $\hat{\mathbf{x}}_I(\omega_j)$ at each frequency will span the same subspace. Fig. 2 shows the eigenspectrum of the broadband interference covariance matrix obtained by performing WIF,

$$\mathbf{R}_I = \frac{1}{J}\sum_{j=1}^{J}E|\hat{\mathbf{x}}_I(\omega_j)\hat{\mathbf{x}}_I^H(\omega_j)| = \frac{1}{J}\sum_{j=1}^{J}E|s_I(\omega_j)|^2\mathbf{b}\mathbf{b}^H \tag{10}$$

which is rank-one in theory. Also shown in the figure is the eigenspectrum of the broadband covariance matrix obtained through averaging the decomposed narrowband covariance matrices, without spatial resampling and presteering. In this simulation WIF focuses 20 frequency points (250-270Hz) to

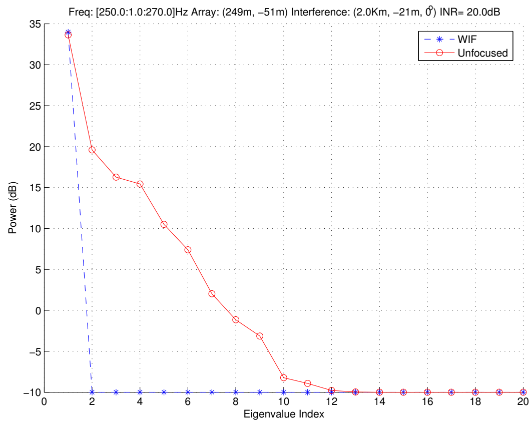

Fig. 2. Dimensionality reduction of WIF

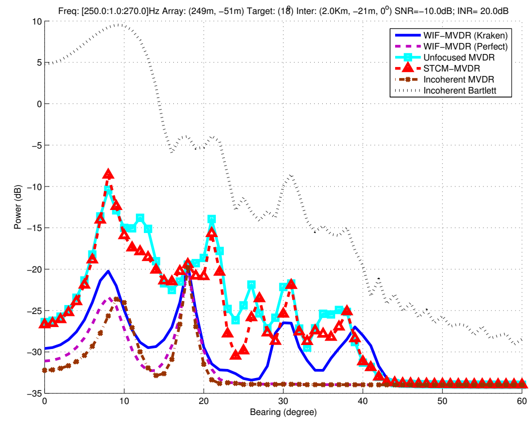

Fig. 3. Spatial spectrum output of WIF-MVDR compared with other methods

the lowest frequency. The plot only shows the energy of the largest 20 eigenvalues. It can be seen that WIF drops the energy of subdominant eigenvectors much more rapidly than usual frequency averaging.

The operation of spatial resampling and presteering is also applied to the target signal. If the target wavefront is planewave, its direction vectors across frequencies become:

$$\hat{\mathbf{x}}_T(\omega_j) = \tilde{s}_T(\omega_j) \exp\left(-j(k_p(\omega_j)\sin\theta_T - k_1(\omega_j))\Delta\mathbf{d}\right) \tag{11}$$

where $\tilde{s}_T(\omega_j)$ is target signal amplitude at frequency ω_j. $k_p(\omega_j)$ is the wavenumber, which is a known quantity. θ_T is target bearing.

Thus after focusing, the received signal (1) becomes:

$$\begin{aligned}\hat{\mathbf{x}}(\omega_j) &= \tilde{s}_T(\omega_j) \exp\left(-j(k_p(\omega_j)\sin\theta_T - k_1(\omega_j))\Delta\mathbf{d}\right) \\ &\quad + \tilde{s}_I(\omega_j)\mathbf{b} + \hat{\mathbf{n}}_j \end{aligned} \tag{12}$$

Forming the broadband covariance matrix:

$$\mathbf{R} = \frac{1}{J}\sum_{j=1}^{J} E[\hat{\mathbf{x}}_j \hat{\mathbf{x}}_j^H] = \mathbf{R}_I + \mathbf{R}_T + \sigma_n^2 \mathbf{I} \tag{13}$$

where $\mathbf{R}_I$ is the interference covariance matrix expressed in (10). $\mathbf{R}_T$ is the target covariance matrix:

$$\mathbf{R}_T = \frac{1}{J}\sum_{j=1}^{J} E|s_T(\omega_j)|^2 \mathbf{v}_j(\theta_T)\mathbf{v}_j(\theta_T)^H \tag{14}$$

where

$$\mathbf{v}_j(\theta) = \exp\left(-j(k_p(\omega_j)\sin\theta - k_1(\omega_j))\Delta\mathbf{d}\right) \tag{15}$$

is the post focusing target signal direction vector.

Now that we have a focused broadband covariance matrix, narrowband beamforming techniques can be applied to estimate target bearing. Because the target signal has different direction vectors for different frequencies, the weights of the minimum variance distortionless response (MVDR) beamformer are designed for each frequency:

$$\mathbf{w}_j(\theta) = \frac{\mathbf{R}^{-1}\mathbf{v}_j(\theta)}{\mathbf{v}_j(\theta)^H \mathbf{R}^{-1}\mathbf{v}_j(\theta)} \tag{16}$$

The broadband spatial spectrum output of WIF-MVDR is:

$$P(\theta) = \sum_j \mathbf{w}_j^H(\theta)\mathbf{R}_j \mathbf{w}_j(\theta) \tag{17}$$

where $\mathbf{R}_j$ is the covariance matrix at frequency ω_j: $\mathbf{R}_j = E[\hat{\mathbf{x}}_j \hat{\mathbf{x}}_j^H]$.

3. SIMULATIONS

To generate the multipath interference signal, the following simulations use the environmental profile of the SWellEx-96 experiment. [7] The β is assumed known as 1.1. Fig. 3 shows the spatial spectrum output of WIF-MVDR compared with other methods. A planewave target signal impinges on a horizontal linear array at 18^o with SNR -10dB. A loud endfire interference from 2km away has an interference-to-noise ratio (INR) 20dB. Several different broadband beamforming methods are tested. The broadband incoherent Bartlett and MVDR methods process each frequency separately and incoherently average the outputs. In the output of incoherent Bartlett method, we can see the interference completely masks the target. The incoherent MVDR (Clairvoyant) method gives very good resolution, but it is impractical because of its requirement for perfect knowledge of interference covariance matrix at each frequency. Note the major interference peak is not at endfire direction due to wavenumber spreading. Both Unfocused MVDR and STCM-MVDR form broadband covariance matrices. The difference is that in doing so unfo-

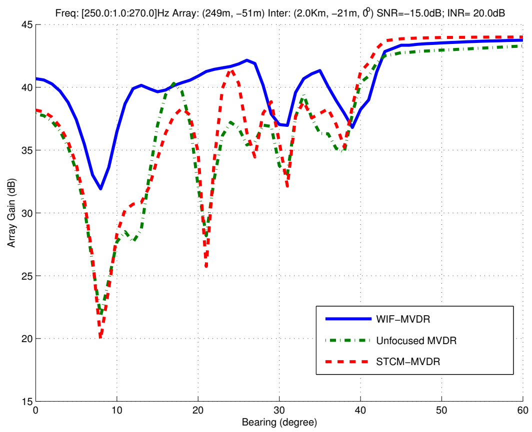

Fig. 4. Array gain of WIF-MVDR

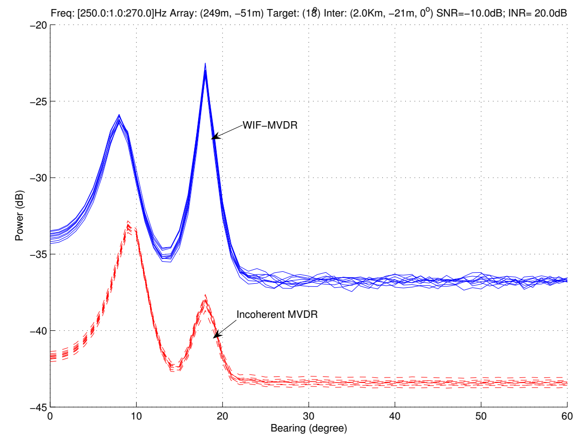

Fig. 5. Finite snapshot performance of WIF-MVDR

cused MVDR simply averages all narrowband covariance matrices, while STCM-MVDR focuses them before averaging. Their outputs clearly reveal the bearing spread of the interference signal. Still, the target is almost masked by the interference.

The WIF-MVDR results are presented with two curves. WIF-MVDR (perfect) use a perfect constant β as the parameter to simulate broadband interfering wavefronts. This eliminates the approximation of waveguide invariant theory. The result is very close to that of broadband incoherent MVDR, which is optimal but unrealizable. WIF-MVDR (Kraken) simulates the broadband interfering wavefronts from normal mode program Kraken. We can see that the target is also identified, but with some sidelobes because of imperfection of β. Overall, WIF gives much improved interference suppression performance over the other methods considered.

In terms of array gain, Fig. 4 shows the performance of WIF-MVDR, unfocused MVDR and STCM-MVDR at SNR -15dB and INR 20dB. For the large part of the bearing range close to endfire, WIF-MVDR outperforms STCM-MVDR and unfocused MVDR by as much as 15dB.

Fig. 5 shows the 10 realizations of spectrum outputs of WIF-MVDR and broadband incoherent MVDR with 25 snapshots at each frequency. This is equivalent to 13s data of 1s FFT length with 50% ovelapping. It can be seen that all outputs of WIF-MVDR identify the target while incoherent broadband MVDR fails to produce its asymptotic performance due to limited snapshots.

4. CONCLUSION

This paper proposed an innovative approach to achieve broadband focusing for multipath signals frequently encountered in oceanic waveguide. The method, waveguide invariant focusing, utilizes the waveguide invariant to reduce the rank of a broadband target signal signature without acoustic field computations. It can be implemented using a moving horizontal linear array. In the paper WIF was applied to focus on the multipath interference which has large bearing spread at near endfire directions. It was shown to significantly improve the interference suppression performance.

5. REFERENCES

[1] H. Hung and M. Kaveh, “Focussing matrices for coherent signal-subspace processing,” *IEEE Transactions on Acoustics, Speech, and Signal Processing*, vol. 36, no. 8, pp. 1272–1281, Aug. 1988.

[2] J. Krolik and D. Swingler, “Multiple broad-band source location using steered covariance matrices,” *IEEE Transactions on Acoustics, Speech, and Signal Processing*, vol. 37, pp. 1481–1494, 1989.

[3] G. L. D’Spain and W. A. Kuperman, “Application of waveguide invariants to analysis of spectrograms from shallow water environments that vary in range and azimuth,” *J. Acoust. Soc. Am.*, vol. 106, pp. 2454–2468, 1999.

[4] A. M. Thode, W. A. Kuperman, G. L. D’Spain, and W. S. Hodgkiss, “Localization using Bartlett matched-field processor sidelobes,” *J. Acoust. Soc. Am.*, vol. 107, no. 1, pp. 278–286, 2000.

[5] T. C. Yang, “Beam intensity striations and applications,” *J. Acoust. Soc. Am.*, vol. 113, no. 3, pp. 1342–1352, 2003.

[6] G. A. Grachev, “Theory of acoustic field invariants in layered waveguides,” *Acoust. Phys.*, vol. 39, pp. 33–35, 1993.

[7] The SWellEx-96 Experiment website. [Online]. Available: http://www.mpl.ucsd.edu/swellex96/